



HAL
open science

Experiments on 'quantum' search and directed transport in microwave artificial graphene

Julian Böhm, Matthieu Bellec, Fabrice Mortessagne, Ulrich Kuhl, Sonja Barkhofen, Stefan Gehler, Hans-Jürgen Stöckmann, Iain Foulger, Sven Gnutzman, Gregor Tanner

► To cite this version:

Julian Böhm, Matthieu Bellec, Fabrice Mortessagne, Ulrich Kuhl, Sonja Barkhofen, et al.. Experiments on 'quantum' search and directed transport in microwave artificial graphene. *Physical Review Letters*, 2015, 114, pp.110501. hal-01070322

HAL Id: hal-01070322

<https://hal.science/hal-01070322>

Submitted on 1 Oct 2014

HAL is a multi-disciplinary open access archive for the deposit and dissemination of scientific research documents, whether they are published or not. The documents may come from teaching and research institutions in France or abroad, or from public or private research centers.

L'archive ouverte pluridisciplinaire **HAL**, est destinée au dépôt et à la diffusion de documents scientifiques de niveau recherche, publiés ou non, émanant des établissements d'enseignement et de recherche français ou étrangers, des laboratoires publics ou privés.

Experiments on ‘quantum’ search and directed transport in microwave artificial graphene

Julian Böhm,¹ Matthieu Bellec,¹ Fabrice Mortessagne,¹ Ulrich Kuhl,^{1,*} Sonja Barkhofen,^{2,3} Stefan Gehler,^{2,4} Hans-Jürgen Stöckmann,² Iain Foulger,⁵ Sven Gnutzman,⁵ and Gregor Tanner⁵

¹*Université Nice Sophia Antipolis, CNRS, Laboratoire de Physique de la Matière Condensée, UMR 7336 Parc Valrose, 06100 Nice, France*

²*AG Quantenchaos, Fachbereich Physik der Philipps-Universität Marburg, D-35032 Marburg, Germany*

³*Applied Physics, University of Paderborn, Warburger Strasse 100, 33098 Paderborn, Germany*

⁴*Department Energy Management and Power System Operation, University of Kassel, D-34121 Kassel, Germany*

⁵*School of Mathematical Sciences, University of Nottingham, University Park, Nottingham NG7 2RD, United Kingdom*

(Dated: October 1, 2014)

A series of quantum search algorithms has been proposed recently providing an algebraic speed-up compared to classical search algorithms from N to \sqrt{N} where N is the number of items in the search space. In particular, devising searches on regular lattices have become popular extending Grover’s original algorithm to spatial searching. Working in a tight-binding setup, it could be demonstrated theoretically, that a search is possible in the physically relevant dimensions 2 and 3 if the lattice spectrum possess Dirac points. We present here a proof of principle experiment implementing wave search algorithms and directed wave transport in a graphene lattice arrangement. The idea is based on bringing localized search states in resonance with an extended lattice state in an energy region of low spectral density - namely at or near the Dirac point. The experiment is implemented using classical waves in a microwave setup containing weakly coupled dielectric resonators placed in a honeycomb arrangement, i.e. artificial graphene. We furthermore investigate the scaling behavior experimentally using linear chains.

PACS numbers: 03.67.Ac,72.80.Vp,03.67.Lx,42.50.Md

Introduction.— Currently, one of the most fruitful branches of quantum information is the field of quantum search algorithms. It started with Grover’s work [1] describing a search algorithm for unstructured databases which has been implemented experimentally in NMR [2, 3] and in optical experiments [4, 5]. More recently, spatial quantum search algorithms have been proposed based on quantum walk mechanism [6, 7]. All these algorithms can achieve up to quadratic speed-up compared to the corresponding classical search. For quantum searches on generic d -dimensional lattices certain restrictions have been observed, however, depending on whether the underlying quantum walk is discrete [8] or continuous [9]. While effective search algorithms for discrete walks on square lattices have been reported for $d \geq 2$ [10, 11], continuous-time quantum search algorithms on the same lattice show speed-up compared to the classical search only for $d \geq 4$ [12].

Experimental implementations of discrete quantum walks need time stepping mechanisms such as laser pulses [13–18]. By switching to a continuous-time evolution based, for example, on tight-binding coupling between sites one can avoid time-discretization in an experiment. It has been shown in [19] that continuous-time quantum search in 2D is indeed possible when performed near the Dirac point in graphene or more generally for lattices with cone structure in the dispersion relation [20], i.e., a linear growth of the density of states (DOS). This effect adds a new dimension to the material properties of

graphene [21, 22] with potential applications in sensing and detection as well as directed charge carrier transport. This may provide new ways of channeling intensity and information across lattices and between distinct sites, such as for single-molecule sensing as described in [23, 24]. In this Letter, we present the first experimental realization of a 2D search in a tight-binding setup based on a microwave experiment using artificial graphene as discussed in [25–27].

In the following, we recapitulate briefly the theory of quantum searching on graphene and describe the experimental setup. We then demonstrate both searching as well as directed transport in graphene-like lattice structures. To explore the scaling behavior with the number of sites, we consider a linear chain demonstrating explicitly the \sqrt{N} scaling.

Theoretical background.— All quantum search algorithms, starting from Grover’s search on an unstructured database, are based on the same principle: the system is setup by bringing an extended state of the (unperturbed) system in resonance with a localized state originating from a perturbation, thereby forming an avoided crossing in the spectrum of resonances. One then uses the 2-level dynamics at the avoided crossing in order to rotate the system from the extended state into the localized state thus ‘finding’ the position of the perturbation [28, 29]. The subtleties in setting up such a search lie in i) choosing an unperturbed system with eigenstates extending uniformly across all sites; ii) finding a suitable

perturbation which carries localized state and iii) working in an energy range with a low density of states making it possible to isolate the two-level crossing from the rest of the spectrum.

In the following, we will focus on continuous-time walks on regular, finite lattices in a tight-binding setup. The entries in the database are represented by the N lattice sites and associate orthonormal states $\{|i\rangle\}_{i=1}^N$ spanning an N dimensional Hilbert (search) space. The system is described by a tight-binding Hamiltonian H_0 with associate eigenstates $\{|e\rangle\}_{e=1}^N$. The extended eigenstates most suitable for a search are those corresponding to reciprocal lattice-vectors at $k = 0$ or near the band edge. Introducing a perturbation of the form $H = H_0 + W$ with W supporting a localized state at the ‘marked site’ being in resonance with a uniform extended state. The interaction at the avoided crossing is controlled by the overlap integral $|\langle i|e\rangle|^2 \approx N^{-1}$, which leads to an energy gap of order $1/\sqrt{N}$. The search is started by preparing the system in an extended state $|e\rangle$. The state then evolves according to $|\psi(t)\rangle = e^{-iHt/\hbar}|e\rangle$ describing a rotation taking place predominantly in the two-dimensional subspace spanned by $|i\rangle, |e\rangle$. Performing a measurement after the system has evolved into $|i\rangle$ at a time $t_c = \mathcal{O}(\sqrt{N})$ completes the search.

For generic lattices, the number of states with energy less than E in d dimensions scales typically as $NE^{d/2}$. One thus expects the first state above the ground state at an energy $E_1 = \mathcal{O}(N^{-2/d})$. An energy separation between the states at the avoided crossing (being at a distance $\mathcal{O}(N^{-1/2})$) and the rest of the spectrum is thus only possible for $d \geq 4$ in the large N limit. Running the search at a Dirac point overcomes this problem; here the energy scaling is reduced to $E_1 = \mathcal{O}(N^{-1/d})$ and searching becomes possible for $d \geq 2$ [19, 20]. In contrast to [19], the perturbation W introduced in this letter is in terms of coupling an additional site to the lattice state $|i\rangle$ with the perturber’s on-site energy tuned to an extended state close to the Dirac point.

Experiments on graphene.— The experimental microwave setup is shown in the inset of Fig. 1. A metallic plate supports ceramic cylinders of height $h = 5$ mm and radius $r = 4$ mm which have a high index of refraction ($n \approx 6$) thus acting as resonators. Microwaves are coupled into the system via antennas, which excite the first transverse electric resonance, called TE_1 , at $\nu_0 \approx 6.65$ GHz of the resonators. The system is closed from above by a metallic top plate at a distance of $h_p = 16$ mm (not shown). We form a ‘graphene flake’ by positioning 216 resonators in a hexagonal lattice, see inset of Fig. 1, thus creating artificial graphene [25–27]. The top plates holds a loop antenna which can be positioned arbitrarily in the xy plane above each resonator. It couples via the magnetic field into the TE_1 mode. For details on the experimental setup and its relations to a tight-binding model refer to Ref. [27]. The reflection

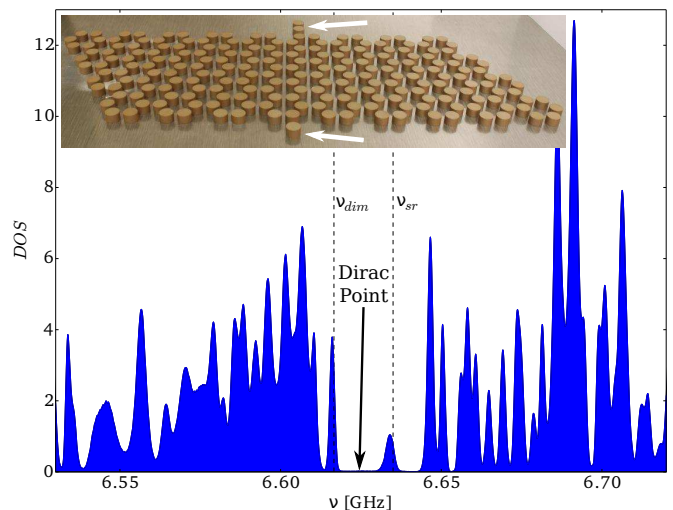


FIG. 1. (color online) The inset is a photograph of the graphene flake including the supporting metallic plate and the perturber resonators at the boundary (white arrows). The graph shows the DOS of the unperturbed flake, i.e. without single resonator and dimer attached. The resonance frequencies of the single resonator ν_{sr} and the dimer ν_{dim} are marked by the dashed vertical lines.

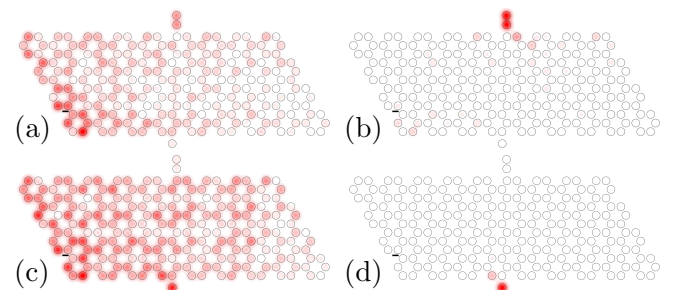


FIG. 2. (color online) (a) and (c): The initial lattice state at $t = 0$ for two different initial frequency ranges is shown. (c) for the range including the dimer frequency ν_{dim} and the lower lattice state ν_l and (d) the range including ν_s and ν_u . (b) and (d) show the illuminated perturber state at the search time $t = T_{dim}$ and T_{sr} , respectively. See Supplemental Material at ... for a video showing the full dynamics (DimerSearchOnGraphene.mp4 and MonomerSearchOnGraphene.mp4).

of the moving antenna at the center of the resonator is proportional to the intensity of the eigenmodes $|\Psi(r_n)|^2$, where n labels the resonator, thus allowing for a determination of the local density of states (LDOS) and by integration the DOS as well. A transmission measurement from the fixed antenna 1 to the movable antenna 2 yields also the phases. Thus, by means of a Fourier transform, we determine the time dependent propagator $P(r_n, t) = |FT(S_{12}(r_n, \nu))|^2$, where S_{12} is the measured transmission spectrum taken at every resonator position r_n of the movable antenna [30, 31]. The DOS for the graphene flake close to the Dirac point is shown in Fig. 1. One can clearly identify two isolated states, which are

extended lattice states. The lower one is denoted by ν_l and the upper one by ν_u . We will use the frequencies of these states near the Dirac point as working points for our search algorithm.

In the next step, we attach two perturbations at the side of the flake, see the inset of Fig. 1. The perturbation in the foreground is a single resonator with eigenfrequency ν_{rs} close to ν_u , the one in the background consists of a dimer, that is, two strongly coupled resonators with its lower frequency ν_{dim} adjusted to ν_l (see also dashed lines in Fig. 1). We have chosen this dimer configuration for having a parameter to fine-tune the frequency ν_{dim} . The perturbations induce new resonance states interacting with the lattice states ν_l and ν_u . The time dependence of the search dynamics can now be demonstrated by Fourier transforming S_{12} in a small frequency window around ν_l or ν_u . Fig. 2(a,c) shows the thus obtained initial state at $t = 0$ for the two different incident states. The state shown in Fig. 2(a) involves only frequencies close to ν_l and ν_{dim} and in Fig. 2(c) only frequencies close to ν_u and ν_s are included. After some time $t = T_{dim}$ ($t = T_{sr}$) the dimer (the single resonator) is illuminated and the perturbation is thus found [see Fig. 2(b,d)]. The search times T_{dim} and T_{sr} are slightly different due to differences in the coupling of the perturbation to the corresponding extended states.

By working near the Dirac point, the search can be extended to an arbitrary number of resonators N in principle; in praxis, the size of our model system is limited due to the overall absorption (quality factor around 1000). A detailed analysis of how the search time scales with N is thus not possible here. We will demonstrate this in a slightly different setup using a linear chain at the end of the Letter.

Our experiment demonstrates that the effect of spatial searching can be achieved in a graphene-like setup with tight-binding interaction. This is encouraging as the model here differs significantly from the theoretical study presented in [19] due to different boundary conditions, experimental uncertainties and absorption. Our results point towards a completely new set of applications in the actual carbon material - graphene - where the limitations due to absorption are less severe. In addition to forming the basis of a storage device with fast searching facility as demonstrated above, the results presented in Fig. 2 can also be interpreted in the framework of directed electron transport. One could use the device as a sensitive switch, where current will be directed either to the upper (dimer) or lower (single resonator) port depending on the Fermi energy.

Spatial quantum search can also be used for communication and ‘quantum state transfer’ [19, 29, 32]. The lattice is perturbed by two equivalent resonators, whose eigenfrequencies are tuned to a single eigenfrequency of the unperturbed lattice. The perturbations are attached at two different positions to the lattice and interact only via

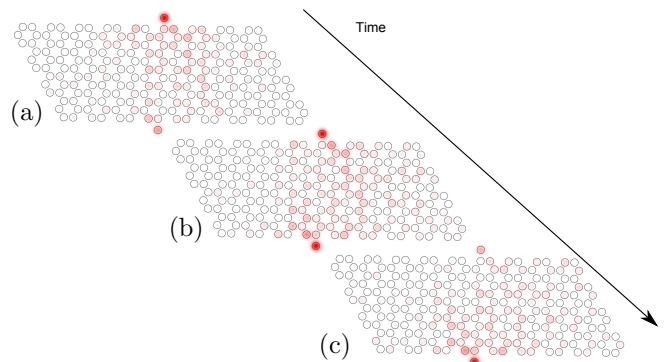


FIG. 3. (color online) Intensity propagation in a graphene flake with two equal perturbing resonators attached. The initial state at $t = 0$ is localized at the upper resonator and is transferred via a lattice state to the state sitting on the opposite resonator. See Supplemental Material at ... for a video showing the full dynamics (StateTransferOnGraphene.mp4).

the lattice state. Launching an initial pulse in the lattice state will illuminate at the same time the two resonators but with reduced brightness. If we, however, prepare the initial state in one of the perturbing resonators and let the system evolve thereafter, the pulse will actually travel from the initial resonator via the lattice to the second resonator. The evolution is presented in Fig. 3. This time the upper resonators [Fig. 3(a)] is illuminated initially, we then go to a state living both in the lattice and on the two perturbing resonators [Fig. 3(b)]. Then the other resonator lights up [Fig. 3(c)] and (nearly) the total amplitude is transferred from one resonator to the other. This opens the way towards directed signal transfer and control in graphene; of course, graphene can not yet be manipulated on a single atom level as would be necessary for making use of the effects described in this letter. Our results may serve as incentive to trigger research efforts.

Experiment on linear chains.— In order to show the \sqrt{N} scaling behavior of the search time in our experimental setup, we go to a simpler, quasi one-dimensional system, a linear chain. Searching is possible here only for small N , as the distance between neighboring resonances scales like N^{-2} and the number of resonances will flood the avoided crossing eventually for large N [19]. However, for small $N < N_{cut}$, the effect can be nicely demonstrated as shown below. A photograph of the unperturbed chain with $N = 11$ resonators is depicted in Fig. 4(a); that is well below the cut-off which is $N_{cut} = 27$ for the setup shown here. The reflection spectrum $1 - |S_{11}|^2$ of this unperturbed chain is given in Fig. 4(b) as a black line (central spectrum), where we observe the 11 resonances of the regular chain. The central frequency for a chain with an odd number of resonators is always at the eigenfrequency of the single resonator and thus does not depend on N . The experimentally measured lattice mode which we use for the wave search realization is superimposed on

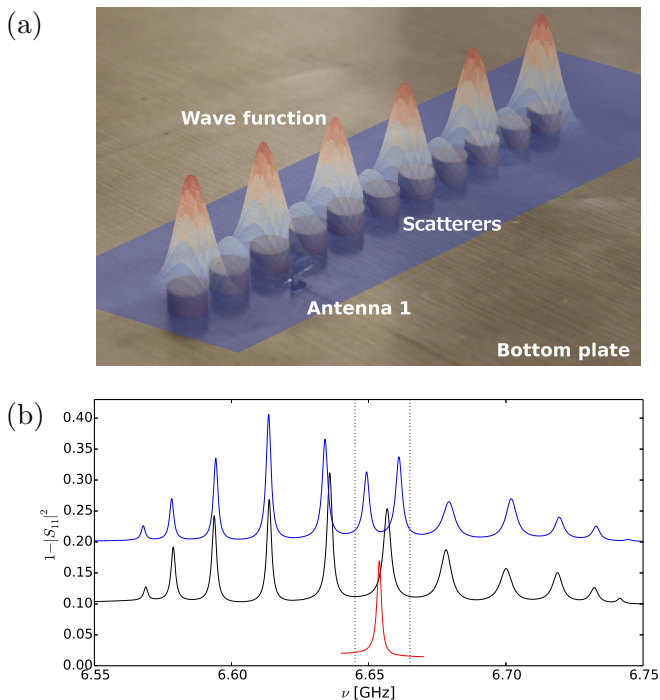


FIG. 4. (color online) (a) Experimental setup showing the linear chain with $N=11$ resonators without perturber. The top plate and antenna are not shown. The wave function corresponding to the central resonance which we use for the wave search is superimposed. (b) Reflection measurement of a single resonator (red, bottom), a regular chain with 11 resonators (black, center), and of the single resonator being attached to the regular chain (blue, top). The dotted lines mark the frequency range used for the Fourier transform to obtain the propagations. The baseline of the spectra are shifted correspondingly.

the photograph. It is the central mode which for an odd number of states is given by $|\Psi(r_n)| = 1/\sqrt{(N+1)/2}$ for n odd and 0 otherwise. Additionally the reflection spectrum measured on a single state is presented (red, lower spectrum). The eigenfrequency matches the central resonance of the unperturbed chain. When attaching a perturber resonator to the chain, we find an additional resonance interact with the lattice state resulting in a resonance splitting (blue, top spectrum). The propagator is calculated by Fourier transforming the frequency range marked by the dotted vertical lines in Fig. 4(b) containing only central mode and the perturber state.

Fig. 5(a) depicts the temporal behavior of the intensity of the whole chain (black line) and of the perturber resonator (red line). The initial state ($t=0$) is adjusted to the maximal amplitude on the lattice. We observe an oscillatory behavior corresponding to a beating between the two states. The search time T_s is given by half the beating time T . The insets show the corresponding intensities of the wave function at the indicated times. We perform the same kind of measurements for different number of

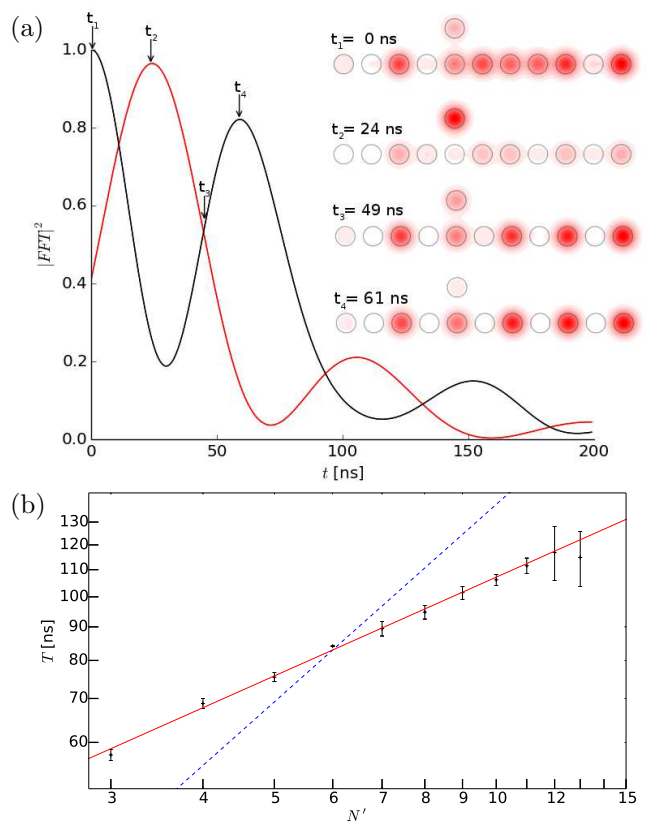


FIG. 5. (color online) (a) The time dependence of the intensity of the chain with 11 resonators (black line) and of the perturber (red line) is shown. The corresponding intensity distribution for specific times are shown as insets. See Supplemental Material at ... for a video showing the full dynamics (DiskSearchOnLinearChain.avi). (b) The beating time as a function of N' is shown. The dashed line corresponds to a linear increase whereas the solid line marks a square root dependence. The errorbars indicate the time difference between different recurrences.

odd sites N ranging from 5 to 27. Fig. 5(b) shows the search time T_s as a function of sites $N' = (N+1)/2$. We observe the predicted $\sqrt{N'}$ behavior.

Conclusion.— We have demonstrated for the first time an experimental realization of ‘quantum’ wave search on an (artificial) graphene lattice. The search is facilitated by bringing a lattice state in resonance with a localized perturber state at an avoided crossing. The effects range from searching perturber states, to addressing particular sites using a frequency scan or initiating a switching behavior and by transferring signals between sites without knowing their positions. This is a proof of principle experiment limited mainly by losses and absorption. Reducing the resonance widths further, i.e., obtaining a better quality factor Q , can be realized using coupled supraconducting cavities (quality factors of about $Q \approx 10^8$ are possible). One can also think of modeling graphene using elastodynamic systems based on silicon ($Q \approx 10^7$).

Acknowledgements.— We would like to acknowledge inspiring discussion with Klaus Richter.

* ulrich.kuhl@unice.fr

- [1] L. K. Grover, *Phys. Rev. Lett.* **79**, 325 (1997).
- [2] I. L. Chuang, N. Gershenfeld, and M. Kubinec, *Phys. Rev. Lett.* **80**, 3408 (1998).
- [3] J. A. Jones, M. Mosca, and R. H. Hansen, *Nature* **393**, 344 (1998).
- [4] N. Bhattacharya, H. B. van Linden van den Heuvell, and R. J. C. Spreeuw, *Phys. Rev. Lett.* **88**, 137901 (2002).
- [5] P. Walther, K. J. Resch, T. Rudolph, E. Schenck, H. Weinfurter, V. Vedral, M. Aspelmeyer, and A. Zeilinger, *Nature* **434**, 169 (2005).
- [6] N. Shenvi, J. Kempe, and K. B. Whaley, *Phys. Rev. A* **67**, 052307 (2003).
- [7] R. Portugal, *Quantum Walks and Search Algorithms* (Springer, 2013).
- [8] Y. Aharonov, L. Davidovich, and N. Zagury, *Phys. Rev. A* **48**, 1687 (1993).
- [9] E. Farhi and S. Gutmann, *Phys. Rev. A* **57**, 2403 (1998).
- [10] A. Ambainis, J. Kempe, and A. Rivosh, in *Proceedings of the Sixteenth Annual ACM-SIAM Symposium on Discrete Algorithms*, SODA '05 (Society for Industrial and Applied Mathematics, Philadelphia, PA, USA, 2005) pp. 1099–1108.
- [11] G. Abal, R. Donangelo, F. I. Marquezino, and R. Portugal, *Math. Structures in Comp. Sci.* **20**, 999 (2010).
- [12] A. M. Childs and J. Goldstone, *Phys. Rev. A* **70**, 022314 (2004).
- [13] M. Karski, L. Förster, J.-M. Choi, A. Steffen, W. Alt, D. Meschede, and A. Widera, *Science* **325**, 174 (2009).
- [14] H. Schmitz, R. Matjeschk, C. Schneider, J. Glueckert, M. Enderlein, T. Huber, and T. Schaetz, *Phys. Rev. Lett.* **103**, 090504 (2009).
- [15] P. Xue, B. C. Sanders, and D. Leibfried, *Phys. Rev. Lett.* **103**, 183602 (2009).
- [16] F. Zähringer, G. Kirchmair, R. Gerritsma, E. Solano, R. Blatt, and C. F. Ross, *Phys. Rev. Lett.* **104**, 100503 (2010).
- [17] A. Schreiber, K. N. Cassemiro, V. Potoček, A. Gábris, P. J. Mosley, E. Andersson, I. Jex, and C. Silberhorn, *Phys. Rev. Lett.* **104**, 050502 (2010).
- [18] A. Schreiber, A. Gábris, P. P. Rohde, K. Laiho, M. Štefaňák, V. Potoček, C. Hamilton, I. Jex, and C. Silberhorn, *Science* **336**, 55 (2012).
- [19] I. Foulger, S. Gnutzmann, and G. Tanner, *Phys. Rev. Lett.* **112**, 070504 (2014).
- [20] A. M. Childs and Y. Ge, *Phys. Rev. A* **89**, 052337 (2014).
- [21] A. H. C. Nero, F. Guinea, N. M. R. Peres, K. S. Novoselov, and A. K. Geim, *Rev. Mod. Phys.* **81**, 109 (2009).
- [22] H.-S. P. Wong and D. Akinwande, *Carbon Nanotube and Graphene Device Physics* (Cambridge University Press, 2011).
- [23] F. Schedin, A. K. Geim, S. V. Morozov, E. W. Hill, P. Blake, M. I. Katsnelson, and K. S. Novoselov, *Nat. Mater.* **6**, 652 (2007).
- [24] T. O. Wehling, K. S. Novoselov, S. V. Morozov, E. Vdovin, M. I. Katsnelson, A. K. Geim, and A. I. Lichtenstein, *Nano Lett.* **8**, 173 (2008).
- [25] U. Kuhl, S. Barkhofen, T. Tudorovskiy, H.-J. Stöckmann, T. Hossain, L. de Forges de Parny, and F. Mortessagne, *Phys. Rev. B* **82**, 094308 (2010).
- [26] M. Bellec, U. Kuhl, G. Montambaux, and F. Mortessagne, *Phys. Rev. Lett.* **110**, 033902 (2013).
- [27] M. Bellec, U. Kuhl, G. Montambaux, and F. Mortessagne, *Phys. Rev. B* **88**, 115437 (2013).
- [28] B. Hein and G. Tanner, *J. Phys. A* **42**, 085303 (2009).
- [29] B. Hein and G. Tanner, *Phys. Rev. Lett.* **103**, 260501 (2009).
- [30] J. Stein, H.-J. Stöckmann, and U. Stoffregen, *Phys. Rev. Lett.* **75**, 53 (1995).
- [31] C. Poli, M. Bellec, U. Kuhl, F. Mortessagne, and H. Schomerus, “Selective enhancement of topologically induced interface states,” Preprint (2014), arXiv:1407.3703.
- [32] G. M. Nikolopoulos and I. Jex, eds., *Quantum State Transfer and Network Engineering* (Springer, 2014).